

# Testing the anisotropy of cosmic acceleration from Pantheon supernovae sample

Z. Q. Sun<sup>1</sup>, F. Y. Wang<sup>1,2</sup> \*

<sup>1</sup>*School of Astronomy and Space Science, Nanjing University, Nanjing 210093, China*

<sup>2</sup>*Key Laboratory of Modern Astronomy and Astrophysics (Nanjing University), Ministry of Education, Nanjing 210093, China*

5 July 2018

## ABSTRACT

In this paper, we study the anisotropy of cosmic acceleration the using Pantheon sample, which includes 1048 spectroscopically confirmed Type Ia supernovae (SNe Ia) covering the redshift range  $0.01 < z < 2.3$ . In hemisphere comparison method, we find the dipole direction is  $(l = 37 \pm 40^\circ, b = 33 \pm 16^\circ)$  with the maximum anisotropy level of  $\delta = 0.136_{-0.005}^{+0.009}$ . From the dipole fitting method, we find that the magnitude of anisotropy is  $A = (3.7_{-3.7}^{+2.5}) \times 10^{-4}$ , and the direction of the dipole  $(l = 329_{-28}^{+101}^\circ, b = 37_{-21}^{+52}^\circ)$  in the galactic coordinate system. The result is weakly dependent on redshift from the redshift tomography analysis. The anisotropy is small and the isotropic cosmological model is an excellent approximation.

**Key words:** cosmology: theory - dark energy

## 1 INTRODUCTION

Observations of Type Ia supernovae (SNe Ia) have revealed that our Universe is undergoing an era of accelerating expansion (Perlmutter et al. 1999; Riess et al. 1998). Observations from cosmic microwave background (CMB; Planck Collaboration et al. 2016), baryon acoustic oscillations (BAO), clusters of galaxies, gamma-ray bursts (GRBs; Wang et al. 2015) and large-scale structure also support the accelerating expansion. Therefore, the  $\Lambda$ -Cold Dark Matter ( $\Lambda$ CDM) model is widely accepted as the standard model in modern cosmology. However, the  $\Lambda$ CDM model also faces some challenges. For example, there exists a large

\* fayinwang@nju.edu.cn(FYW)

bulk-flow velocity at scales up to about  $100h^{-1}$  Mpc (Lavaux et al. 2010). The “great cold spot” on CMB sky map (Vielva et al. 2004), alignment of polarization directions of quasars in large scale (Hutsemékers et al. 2005), anisotropic distribution of gamma-ray bursts (Gan, Zou & Dai 2016) and spatial variation of the fine structure constant (King et al. 2012; Mariano & Perivolaropoulos 2012) show that the Universe may be anisotropic.

SNe Ia have been widely used to study the possible anisotropy of cosmic acceleration. Antoniou & Perivolaropoulos (2010) firstly used the hemisphere comparison method to search for a preferred axis from the Union2 data set. They found that the expansion rate reaches its maximum in a certain direction. Cai & Tuo (2012) found a similar result in the  $w$ CDM model. Wang & Wang (2014) firstly used SNe Ia and GRBs to study the anisotropic expansion. They found the dipolar anisotropy is more significant at low redshift from the redshift tomography analysis. Meanwhile, several groups have applied the hemisphere comparison method and dipole fitting method to search for preferred direction of cosmic expansion (Mariano & Perivolaropoulos 2012; Cai et al. 2013; Zhao et al. 2013; Yang et al. 2014; Javanmardi et al. 2015; Jimenez et al. 2015; Chang & Lin 2015; Lin et al. 2016a,b; Chang et al. 2017). Sun & Wang (2018) compared the results derived from different SNe Ia samples and found that the anisotropic distribution of SNe Ia coordinates can cause dipole directions and make dipole magnitude larger. Although the magnitude of isotropy is small enough such that the  $\Lambda$ CDM model is an excellent approximation, an anisotropic cosmological model cannot be ruled out. Theoretically, some anisotropic cosmological models have been proposed (Campanelli et al. 2011; Mariano & Perivolaropoulos 2012; Chang et al. 2014; Wang & Wang 2018).

Recently, Scolnic et al., (2018) have compiled a larger SNe Ia sample (called Pantheon) than JLA sample (Jones et al. 2018). Pantheon sample consists 1048 SNe Ia covering the redshift range  $0.01 < z < 2.3$ . The coordinates of SNe Ia in Pantheon sample distribute more uniformly than previous samples, which is important to study the anisotropic expansion (Sun & Wang 2018). In this paper, we investigate the anisotropy of cosmic acceleration using the Pantheon sample. The hemisphere comparison method and dipole fitting method are used.

The paper is organized as follows. In the next section, we introduce the Pantheon sample and methods. The results are given in section 3. The summary is given in section 4.

## 2 THE PANTHEON SAMPLE AND METHODS

### 2.1 The Pantheon sample

Scolnic et al., (2018) compiled the Pantheon sample consisting 1048 SNe Ia covering the redshift range  $0.01 < z < 2.3$ . This sample contains 276 SNe Ia discovered by the Pan-STARRS1 Medium Deep Survey, and SNe Ia from SDSS, SNLS, various low- $z$  and HST samples. The distribution of SNe Ia in the galactic coordinates is shown in Fig. 1. The luminosity distance is

$$D_L(z) = (1+z) \int_0^z \frac{dz'}{E(z')}. \quad (1)$$

In the flat  $\Lambda$ CDM model,  $E(z)$  is

$$E^2(z) = \Omega_{m0}(1+z)^3 + (1 - \Omega_{m0}), \quad (2)$$

where  $\Omega_{m0}$  is the matter density.

The  $\chi^2$  for SNe Ia is obtained by comparing theoretical distance modulus

$$\mu_{\text{th}}(z) = 5 \log_{10}(D_L(z)) + \mu_0, \quad (3)$$

with

$$\mu_0 = 42.38 - 5 \log_{10} h. \quad (4)$$

The value of  $\Omega_{m0}$  is determined by minimizing the value of  $\chi^2$  with observed  $\mu_{\text{obs}}$

$$\chi_{\text{SN}}^2(\Omega_{m0}, \mu_0) = \sum_{i=1}^{1048} \frac{(\mu_{\text{obs}}(z_i) - \mu_{\text{th}}(\Omega_{m0}, \mu_0, z_i))^2}{\sigma_{\mu}^2(z_i)}. \quad (5)$$

We can expand  $\chi_{\text{SN}}^2$  with respect to  $\mu_0$  (Nesseris & Perivolaropoulos 2005)

$$\chi_{\text{SN}}^2 = A - 2\mu_0 B + \mu_0^2 C, \quad (6)$$

here

$$\begin{aligned} A &= \sum_{i=1}^{1048} \frac{(\mu_{\text{obs}}(z_i) - \mu_{\text{th}}(z_i, \mu_0 = 0))^2}{\sigma_{\mu}^2(z_i)}, \\ B &= \sum_{i=1}^{1048} \frac{\mu_{\text{obs}}(z_i) - \mu_{\text{th}}(z_i, \mu_0 = 0)}{\sigma_{\mu}^2(z_i)}, \\ C &= \sum_{i=1}^{1048} \frac{1}{\sigma_{\mu}^2(z_i)}. \end{aligned}$$

The value of Eq. (6) has a minimum for  $\mu_0 = B/C$  at

$$\tilde{\chi}_{\text{SN}}^2 = \chi_{\text{SN},\text{min}}^2 = A - B^2/C, \quad (7)$$

which is not dependent on  $\mu_0$ .

## 2.2 Hemisphere comparison method

The hemisphere comparison method has been widely used in searching for a preferred direction of cosmic expansion (Antoniou & Perivolaropoulos 2010; Yang et al. 2014). For estimating  $\Omega_{m0}$  in  $\Lambda$ CDM model, we can define (Antoniou & Perivolaropoulos 2010)

$$\delta = \frac{\Delta\Omega_{m0}}{\bar{\Omega}_{m0}} = \frac{\Omega_{m0,u} - \Omega_{m0,d}}{(\Omega_{m0,u} + \Omega_{m0,d})/2}, \quad (8)$$

where the subscripts  $u$  and  $d$  represent the best parameter fitting value in the ‘up’ and ‘down’ hemispheres, respectively. We search for axes that maximize  $\delta$  by first evaluating  $\delta$  on randomly chosen axes, then using that axis with maximized  $\delta$  as the initial value for the Nelder-Mead method. the number of data points per hemisphere is approximate 500, we choose 500 axes in this work. Since the hemisphere comparison approach is not pretty fine and sensitive enough to particular types of anisotropy (Mariano & Perivolaropoulos 2012), it is just a rough estimation of the global property.

## 2.3 Dipole fitting method

Mariano & Perivolaropoulos (2012) firstly applied this method to anisotropic study using SNe Ia. we define the distance moduli with dipole  $\mathbf{A}$  and monopole  $B$  as

$$\tilde{\mu}_{th} = \mu_{th}(1 - \mathbf{A} \cdot \hat{\mathbf{n}} + B), \quad (9)$$

where  $\tilde{\mu}_{th}$  is the theoretical value of distance modulus with dipolar direction dependence, and  $\hat{\mathbf{n}}$  is the unit vector pointing at the corresponding SN Ia.  $\hat{\mathbf{n}}$  can be expressed as

$$\hat{\mathbf{n}} = \cos(b) \cos(l) \hat{\mathbf{i}} + \cos(b) \sin(l) \hat{\mathbf{j}} + \sin(b) \hat{\mathbf{k}}. \quad (10)$$

Then the projection is

$$\mathbf{A} \cdot \hat{\mathbf{n}} = \cos(b) \cos(l) A_x + \cos(b) \sin(l) A_y + \sin(b) A_z. \quad (11)$$

The best-fitting dipole and monopole parameters can be derived by minimizing  $\chi_{SN}^2$ . The likelihood of the fitted parameters and the significance of dipole magnitude are derived from Markov Chain Monte Carlo (MCMC) sampling, similar to Sun & Wang (2018).

We construct three types of Monte Carlo samples, which are obtained with distance moduli and coordinates replaced with different synthetic data while keeping redshifts and other properties unchanged.

(i) For the first type of sample,  $\mu_{obs}$  is replaced with synthetic data subject to Gaussian distribution with  $\mu_{obs}$  as the mean value, and  $\sigma$  as the standard deviation, where  $\sigma$  is the

error bar of  $\mu_{\text{obs}}$ . Therefore, we assume the observational results of distance moduli are unbiased. The coordinates remain unchanged.

(ii) For the second type of sample,  $\mu_{\text{obs}}$  is replaced with synthetic data generated by the same way as the first type, but with  $\mu_{\text{obs}}$  as the mean value, thus assuming underlying isotropy in the redshift-distance relation. The coordinates remain unchanged.

(iii) In the third type of sample,  $\mu_{\text{obs}}$  is replaced with synthetic data generated by the same way as the second type, thus assuming underlying isotropy in the redshift-distance relation. In addition, coordinates are replaced with randomly generated coordinates uniformly distributed on the celestial sphere.

For convenience, these three types of samples are called “unbiased”, “isotropic” and “random” samples, respectively. Likelihood distributions of the fitted parameters are approximated by the frequency distribution of “unbiased” samples. The significance of dipole magnitude is defined as the probability of the best-fitting dipole magnitude being larger than that of an arbitrary data set in “isotropic” samples.

### 3 RESULTS

We apply the hemisphere comparison method using the Pantheon sample. The direction of the largest  $\delta$  is ( $l = 37 \pm 40^\circ, b = 33 \pm 16^\circ$ ). The maximum anisotropy level is  $\delta_{\text{max}} = 0.136_{-0.005}^{+0.009}$ . Fig. 2 shows the distribution of  $\delta$ . The star gives the direction of the largest  $\delta$ , and the circle gives the error range.

We also apply the hemisphere comparison method for “isotropic” samples. We get a maximum anisotropy level of  $\delta_{\text{max}} = 0.133_{-0.036}^{+0.037}$ . Using a similar definition as we introduced before, we can get the significance of maximum anisotropy level  $\delta_{\text{max}}$  to be 83.6 per cent. For “random” sample, we get a maximum anisotropy level of  $\delta_{\text{max}} = 0.121_{-0.023}^{+0.028}$ . The distribution of maximum anisotropy level  $\delta_{\text{max}}$  in “isotropic” and “random” samples are shown in Fig. 3.

Further, we explore the possible redshift dependence of the anisotropy. We use a redshift tomography of the data and take the same procedure as before for all the following redshift bins: 0-0.1, 0-0.2, 0-0.3, 0-0.4, 0-0.6, 0-2.3. The results of redshift tomography analysis using hemisphere comparison method are shown in Table 1. The redshift tomography analysis shows that the preferred axes are all located in a relatively small part of the North Galactic Hemisphere, which is consistent with the result of from the Constitution sample (Sun & Wang 2018).

We also study the anisotropy of cosmic acceleration using the dipole fitting method. We find the direction of the dipole is  $(l = 329^{+101}_{-28}, b = 37^{+52}_{-21})$ , which is shown as the circle in Fig. 4. The scatter plot shows fitted dipole directions and magnitudes of “unbiased” samples. The values of the dipole and monopole magnitudes are  $A = (3.7^{+2.5}_{-3.7}) \times 10^{-4}$ , and  $B = (-1.3 \pm 1.6) \times 10^{-4}$ . The statistical significance of the dipole is 47.0 per cent, which is less than  $1\sigma$ . Fig. 5 shows the best-fitting results using the dipole fitting method. For “random” samples, best-fitting dipole directions are evenly distributed on the celestial sphere. The dipole vectors  $\mathbf{A}$  fit well with a spherically symmetric multivariate Gaussian distribution centring at the origin. The mean value is  $\mu = 0$  and standard deviation is  $\sigma = 1.8 \times 10^{-4}$  for each Cartesian components. The monopole  $B$  are also normally distributed, centring at  $B = 0$ . The standard deviation is  $\sigma = 1.0 \times 10^{-4}$ .

Similar to the hemisphere comparison method, we also perform the redshift tomography analysis for this method. The redshift bins are the same as above. The results of redshift tomography analysis using dipole fitting method are shown in Table 2 and Fig. 6. The redshift tomography analysis shows that the preferred axes are all located in a relatively small part of the Hemisphere, except for the first bin. Meanwhile, the statistical significance of the dipole is similar. To examine the anisotropy of the coordinate distribution of the Pantheon sample, we calculate ‘sample counts’ of data points in hemispheres centred at randomly given points. In Fig. 7, we plot ‘mean absolute deviations’ of those sample counts, along with dipole directions of “isotropic” samples. We find that dipole directions “isotropic” samples tend to concentrate in places where sample counts deviate from the average most.

## 4 SUMMARY

From some observations, there seemingly exists some indications for a cosmological preferred axis (Perivolaropoulos 2014). If such a cosmological preferred axis indeed exists, one has to consider an anisotropic cosmological model as a realistic model, instead of the standard cosmological model.

In this paper, we investigate the existence of anisotropy of the Universe by employing the hemisphere comparison method and the dipole fitting method using the Pantheon sample. For the hemisphere method, we use the value of  $\Omega_M$  to quantify the anisotropy level. The dipole direction is  $(l = 37 \pm 40, b = 33 \pm 16)$ . The maximum anisotropy level is  $\delta_{\max} = 0.136^{+0.009}_{-0.005}$ . For the dipole fitting method, we find the direction of the dipole

is ( $l = 329_{-28}^{+101}$ ,  $b = 37_{-21}^{+52}$ ). The values of the dipole and monopole magnitudes are  $A = (3.7_{-3.7}^{+2.5}) \times 10^{-4}$ ,  $B = (-1.3 \pm 1.6) \times 10^{-4}$ . The statistical significance of the dipole is 47.0 per cent, which is less than  $1\sigma$ . Finally, the redshift tomography analysis is used to explore the possible redshift dependence of the anisotropy. From Tables 1 and 2, we find that the result is weakly dependent on redshift.

## ACKNOWLEDGEMENTS

We thank the anonymous referee for constructive comments. We thank D. M. Scolnic for providing the Pantheon sample. This work is supported by the National Basic Research Program of China (973 Program, grant No. 2014CB845800) and the National Natural Science Foundation of China (grants 11422325 and 11373022), the Excellent Youth Foundation of Jiangsu Province (BK20140016).

## REFERENCES

- Antoniu I., erivolaropoulos L., 2010, *J. Cosmology Astropart. Phys.*, 12, 12
- Cai R., Tuo Z., 2012, *J. Cosmology Astropart. Phys.*, 2012, 6
- Cai R. G., Ma Y. Z., Tang B., Tuo Z. L., 2013, *Phys. Rev. D*, 87, 123522
- Campanelli L., Cea P., Fogli G. L., Marrone A., 2011, *Phys. Rev. D*, 83, 103503
- Chang Z., Li X., Lin H.-N., Wang S., 2014, *Eur. Phys. J. C*, 74, 2821
- Chang Z., Lin H. N., 2015, *MNRAS*, 446, 2952
- Chang Z., Lin H. N., Sang Y., Wang S., 2017, arXiv:1711.11321
- Deng H. K., Wei H., 2018, ArXiv e-prints, arXiv:1804.03087
- Deng H. K., Wei H., 2018, ArXiv e-prints, arXiv:1806.02773
- Gan L. X., Zou Y. C., Dai Z. G., 2016, *Chinese Astron. Astrophys.*, 40, 12
- Hutsemékers D., Cabanac R., Lamy H., Sluse D., 2005, *A&A*, 441, 915
- Javanmardi B., Porciani C., Kroupa P., Pflamm-Altenburg J., 2015, *ApJ*, 810, 47
- Jimenez J. B., Salzano V., Lazkoz R., 2015, *Phys. Lett. B*, 741, 168
- Jones D., et al., 2018, *ApJ*, 857, 51
- King J. A., Webb J. K., Murphy M. T., Flambaum V. V., Carswell R. F., Bainbridge M. B., Wilczynska M. R., Koch F. E., 2012, *MNRAS*, 422, 3370
- Lavaux G., Tully R. B., Mohayaee R., Colombi S., 2010, *ApJ*, 709, 483
- Lin H. N., Wang S., Chang Z., Li X., 2016, *MNRAS*, 456, 1881

- Lin H. N., Li X., Chang Z., 2016, MNRAS, 460, 617
- Mariano A., Perivolaropoulos L., 2012, Phys. Rev. D, 86, 083517
- Nesseris S., Perivolaropoulos L., 2005, Phys. Rev. D, 72, 123519
- Perivolaropoulos L., 2014, Galaxies, 2, 22
- Perlmutter S., et al., 1999, ApJ, 517, 565
- Planck Collaboration XIII, 2016, A&A, 594, A13
- Riess A. G., et al., 1998, AJ, 116, 1009
- Scolnic D., et al., 2018, arXiv: 1710.00845
- Sun Z. Q., Wang F. Y., 2018, arXiv: 1804.05191
- Vielva P., et al., 2004, ApJ, 609, 22
- Wang F. Y., Dai Z. G., Liang E. W., 2015, New Astronomy Reviews, 67, 1
- Wang J. S., Wang F. Y., 2014, MNRAS, 443, 1680
- Wang Y. Y., Wang F. Y., 2018, MNRAS, 474, 3516
- Yang X., Wang F. Y., Chu Z., 2014, MNRAS, 437, 1840
- Zhao W., Wu P., Zhang Y., 2013, International Journal of Modern Physics D, 22, 1350060

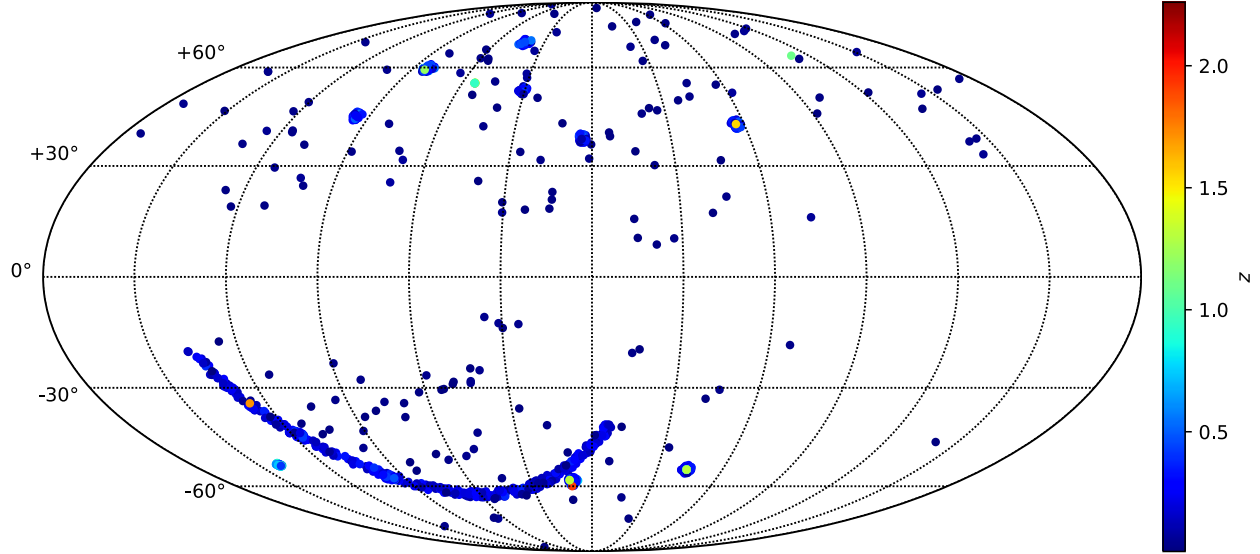


**Table 1.** Redshift tomography results using hemisphere comparison method.

Redshift Range	Data Number	$l$	$b$	$\delta$
$z \leq 0.1$	211	$171^\circ$	$34^\circ$	1.04
$z \leq 0.2$	411	$-47^\circ$	$37^\circ$	0.54
$z \leq 0.3$	630	$-9^\circ$	$50^\circ$	0.38
$z \leq 0.4$	766	$28^\circ$	$43^\circ$	0.23
$z \leq 0.6$	886	$16^\circ$	$36^\circ$	0.18
$z \leq 2.3$	1048	$37^\circ$	$33^\circ$	0.14

**Table 2.** Redshift tomography results using dipole fitting method.

Redshift Range	Data Number	$l$	$b$	$A$	$B$
$z \leq 0.1$	211	$307^\circ$	$25^\circ$	$1.3 \times 10^{-3}$	$-3.6 \times 10^{-4}$
$z \leq 0.2$	411	$296^\circ$	$30^\circ$	$7.7 \times 10^{-4}$	$-3.4 \times 10^{-4}$
$z \leq 0.3$	630	$289^\circ$	$21^\circ$	$9.5 \times 10^{-4}$	$-4.1 \times 10^{-4}$
$z \leq 0.4$	766	$306^\circ$	$26^\circ$	$6.3 \times 10^{-4}$	$-2.6 \times 10^{-4}$
$z \leq 0.6$	886	$320^\circ$	$24^\circ$	$5.1 \times 10^{-4}$	$-1.9 \times 10^{-4}$
$z \leq 2.3$	1048	$329^\circ$	$37^\circ$	$3.7 \times 10^{-4}$	$-1.3 \times 10^{-4}$


**Figure 1.** The distribution of Pantheon sample in the galactic coordinates.

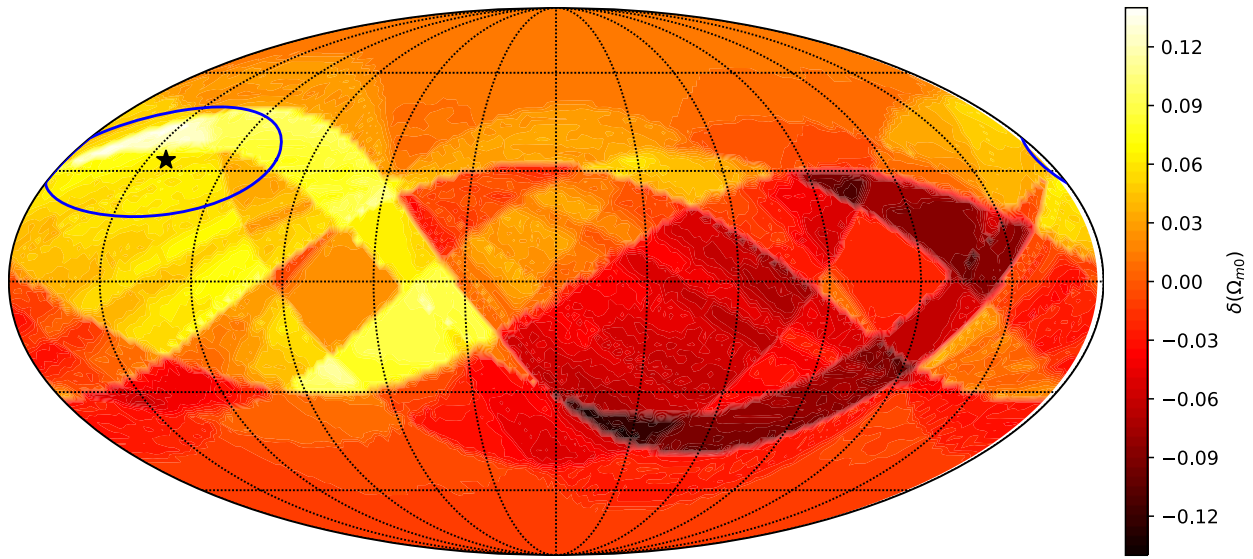


**Figure 2.** The distribution of the hemispherical asymmetry  $\delta = \frac{\Omega_{m0,u} - \Omega_{m0,d}}{(\Omega_{m0,u} + \Omega_{m0,d})/2}$ . The star marks the direction of the largest  $\delta$ , and the circle shows the error range.

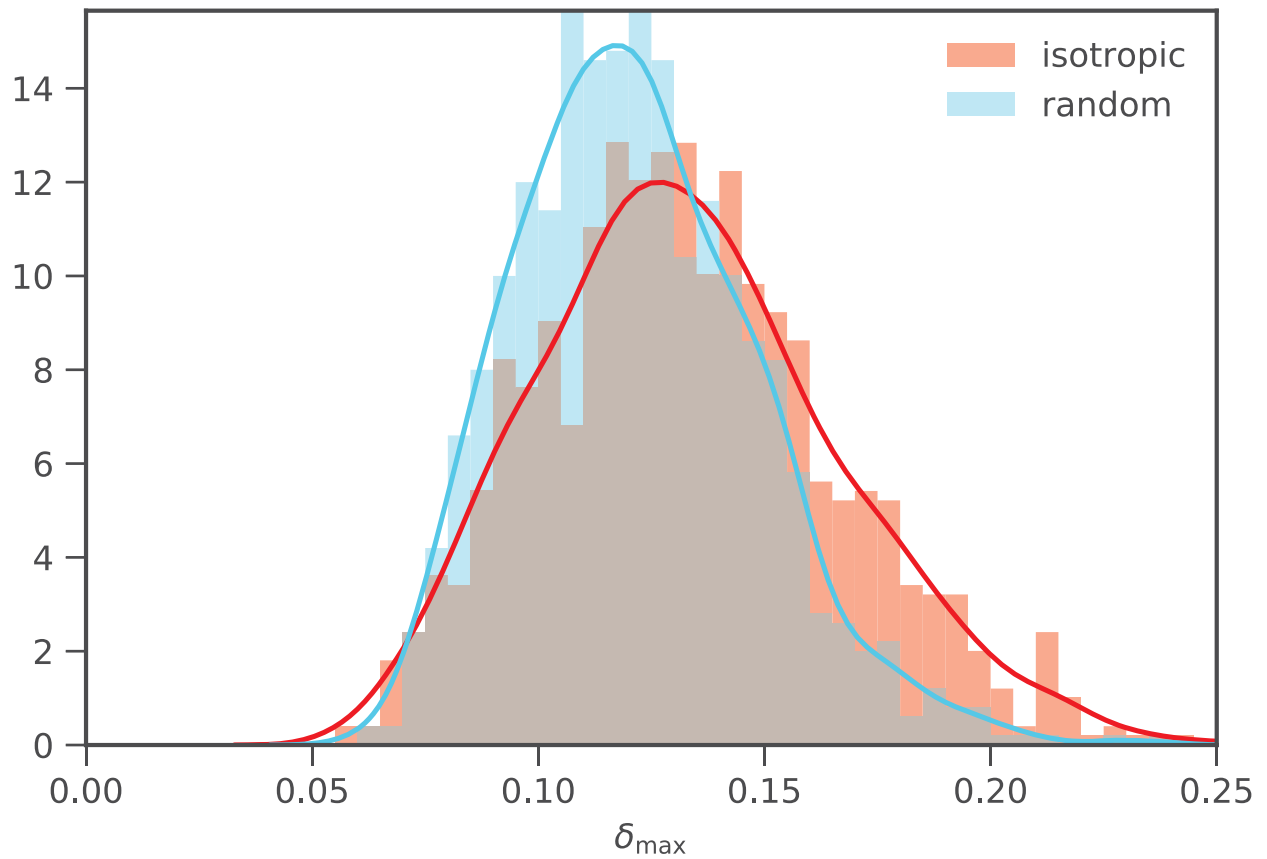


**Figure 3.** Histogram and kernel density plot of maximum anisotropy level  $\delta_{\max}$  for “isotropic” and “random” samples.

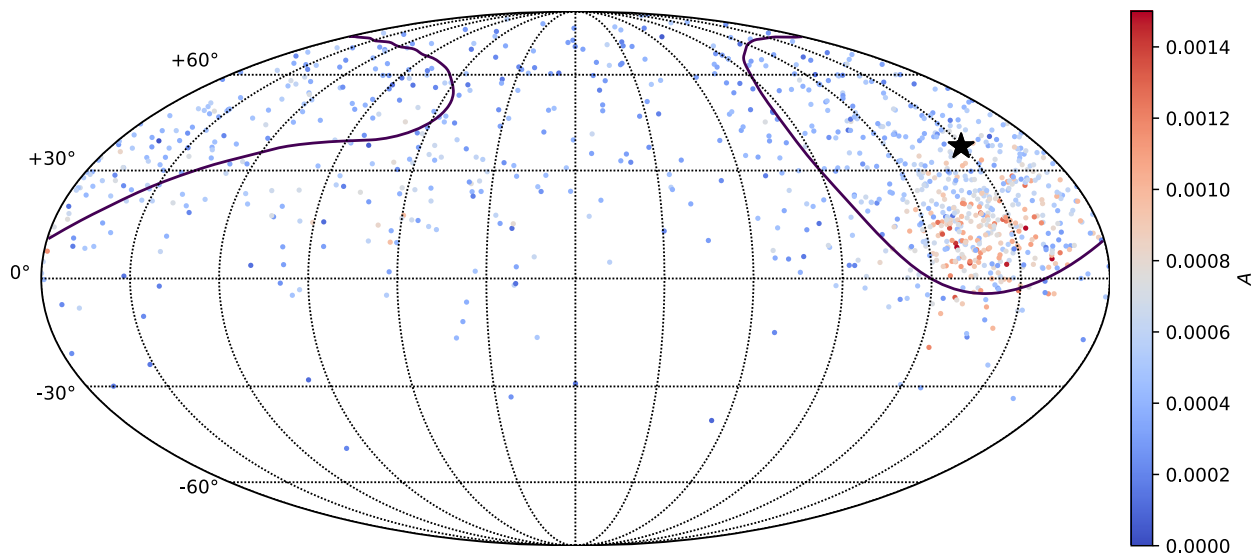


**Figure 4.** Best-fitting dipole direction (star) and the  $1\sigma$  error range of the Pantheon sample. Scatter points represent dipole fitting results of “unbiased” samples.

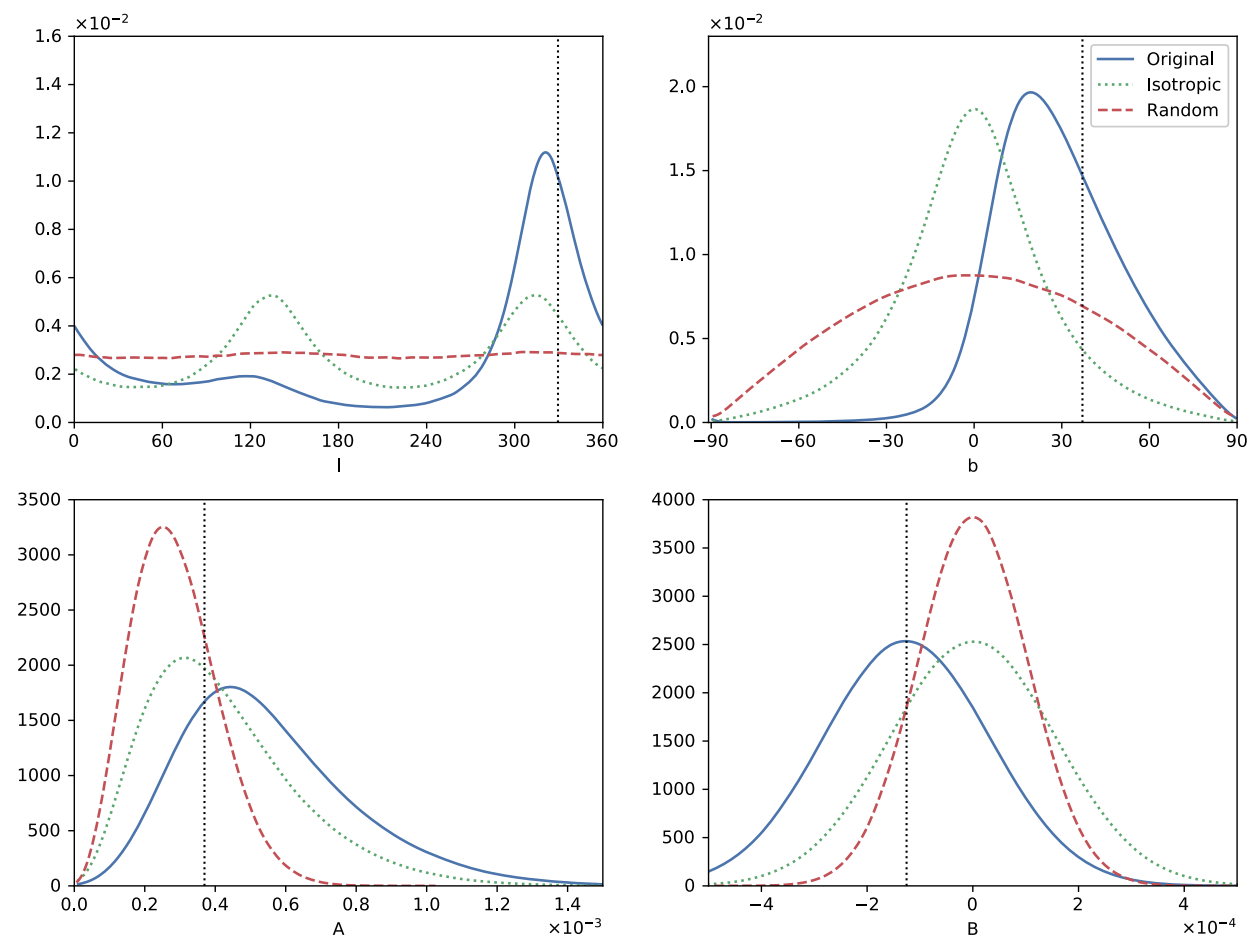


**Figure 5.** The marginalized likelihoods for dipole  $A$ , monopole  $B$  and  $(l, b)$ . Blue, green and orange lines show the results for the Pantheon sample, “isotropic” sample and “random” samples, respectively. The black vertical lines represent best-fitting values.

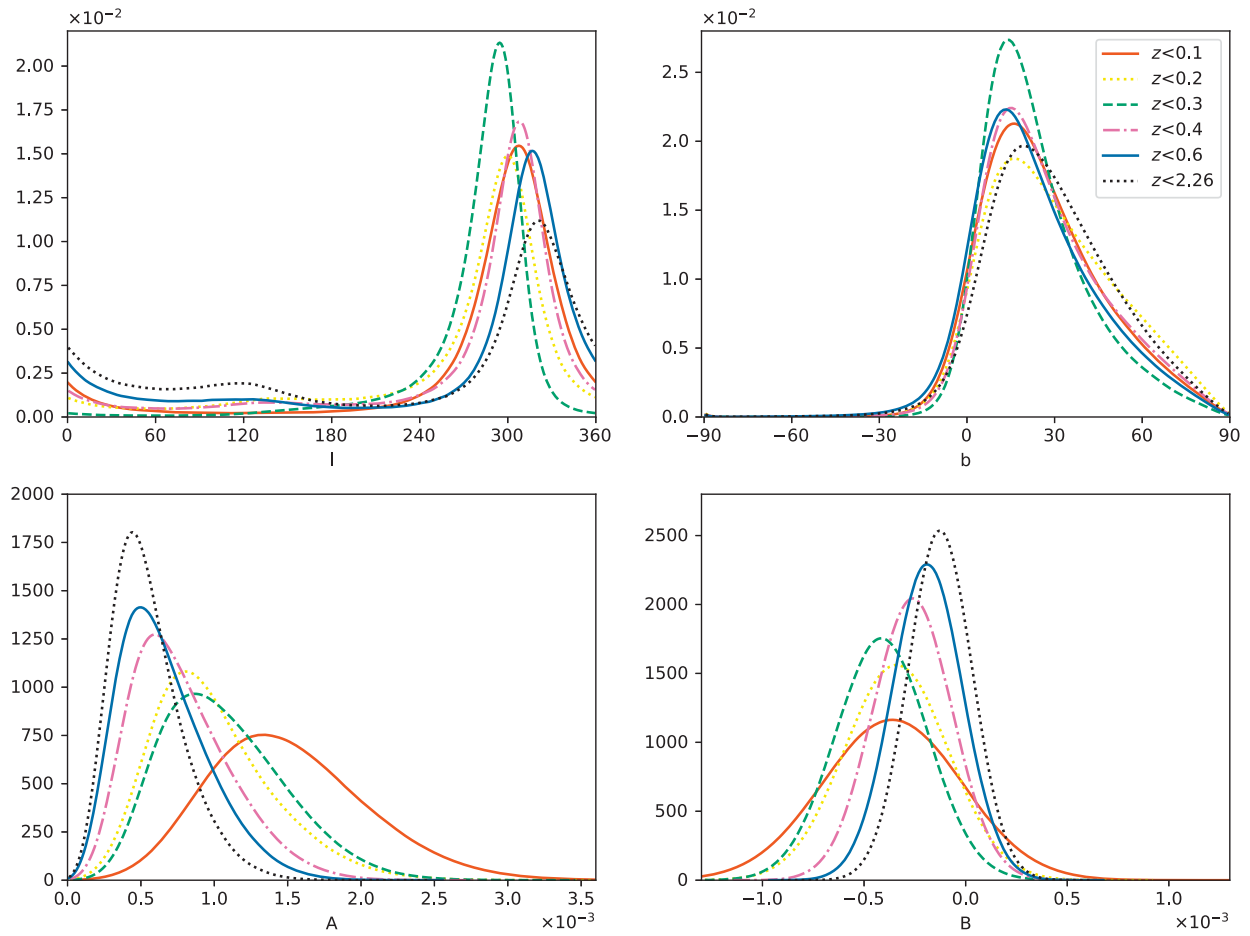


**Figure 6.** Marginalized likelihoods of dipole  $A$ , monopole  $B$  and  $(l, b)$  for different redshift ranges of the Pantheon sample.

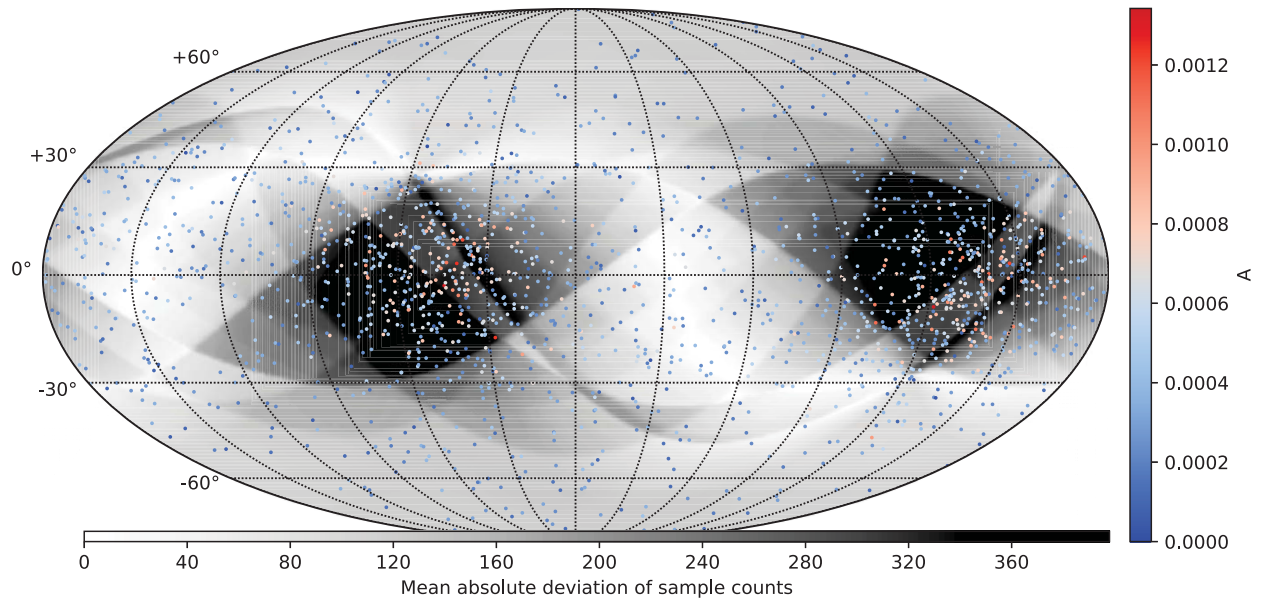


**Figure 7.** Sample count and dipole distribution of the Pantheon samples. The contour shows mean absolute deviations, which represent how far the sample density near a specific point differs from the average density.